Energy Analysis of Eco-Driving Maneuvers on Electric Vehicles

Edwin Solano Araque, Guillaume Colin, Guy-Michel Cloarec, Ahmed Ketfi-Cherif, Yann Chamaillard

HAL Id: hal-01934608
https://univ-orleans.hal.science/hal-01934608

Submitted on 26 Nov 2018

Energy Analysis of Eco-Driving Maneuvers on Electric Vehicles

Edwin Solano Araque *,** **Guillaume Colin** **
Guy-Michel Cloarec * **Ahmed Ketfi-Cherif** *
Yann Chamaillard **

* *Renault S.A.S, France (e-mail: edwin.e.solano-araque@renault.com;
guy-michel.cloarec@renault.com; ahmed.ketfi-cherif@renault.com)*
** *Univ. Orléans, PRISME, EA 4229, F45072, Orléans, France
(e-mail: guillaume.colin@univ-orleans.fr;
yann.chamaillard@univ-orleans.fr)*

Abstract: We present an approach allowing us to compare the energy consumption of an electric vehicle (EV) in different maneuvers of driving scenarios. This approach is used in order to estimate the potential of Eco-driving for reducing EV consumption, and also to analyze where this gain comes from. Drivability constraints were taken into account in the study. We present energy loss distribution among the different components of the vehicle. In simulations, we considered cruising, acceleration and deceleration scenarios in urban driving. Results seem to show that reducing driver aggressiveness on accelerations is the main factor in reducing EV consumption in urban settings.

Keywords: Electric vehicles (EV), Eco-driving, Range, Driving Style, Energy consumption reduction, Drivability

1. INTRODUCTION

In a context where there is a social demand for environmental protection (Miyatake et al. (2011)), reducing greenhouse gases (GHG) and improving air quality (which implies reducing atmospheric pollutant emissions) are becoming more and more relevant topics. The former is usually associated with climate change and the latter with public health.

Transport represents about a quarter of GHG emissions in Europe and is the main cause of air pollution in cities. Road transport is responsible for over 70% of GHG associated to transport, so special efforts must be made in this area. Electric Vehicles (EV) seem to be a well adapted solution for reducing the environmental impact of transport and hence responding to the ecological objectives of many states.

However, there are still some electro-mobility barriers that must be overcomed for EV to become an acceptable solution for mobility for the general public. One obstacle to the adoption of EVs is their limited driving range. There are several ways for improving EV driving range, among which: using fuel-based Range Extended Electric Vehicles (REEV) (Wahono et al. (2015)), increasing battery capacity (Mruzek et al. (2016)), reducing aerodynamic drag and component energy losses, and adopting an energy economic driving style (Mruzek et al. (2016); Badin et al. (2013)). The latter approach is known as Eco-driving (E-D).

E-D has been widely studied in the literature. The notions associated to the definition of E-D vary considerably from one study to another, however. For example, Sivak and Schoettle (2012) include in their E-D definition vehicle selection and maintenance, as well as route selection and vehicle load. Another divergence is the fact that some authors consider that E-D must be executed in a given time (e.g. Mensing et al. (2014); Maamria et al. (2017); Miyatake et al. (2011)), while others consider that an Eco-driver would accept a trade-off between energy consumption and trip time (e.g. Mensing (2013); Saerens (2012); Mruzek et al. (2017)).

It is worth noting that E-D potential and adequate operation are drive train specific (Mensing (2013)). Therefore, E-D strategies that work well on conventional or hybrid vehicles may not necessarily have the same performance on EV. Many authors have proposed approaches to achieve EV specific E-D operation (e.g. Mensing (2013); Dib et al. (2014); Miyatake et al. (2011)).There is, however, a need for a deeper understanding of the sources of energy gains. In Mruzek et al. (2016), the authors present an analysis of the impact of certain parameters on EV range. We consider that it is possible to take this analysis further by directly considering where the energy goes during each maneuver.

In order to better understand why and how E-D improves energy consumption in EV, we have developed an energy model, taking into account separately different loss sources (section 2). Section 3 describes the framework we determined to compare, in a rigorous systematic manner, different scenarios where E-D is applied to a greater or lesser extent; in particular, we have considered independently two techniques that will be explained later on: *slow down* (SDn) and *driver aggressiveness variation* (DAV), in acceleration and in deceleration, in response to a given driving scenario; we also present the results of some simulations for urban driving. Finally, in section 4 we discuss our results and present some perspectives for future research.

The main contributions of our work are the analysis on losses distribution among the different vehicle components on E-D maneuvers, the proposition of a methodology for fairly comparing several E-D strategies and the fact of considering drivability constraints when asserting the E-D potential.

2. ELECTRIC VEHICLE MODELING FOR ECO-DRIVING ANALYSIS

The vehicle considered in our study is a Renault Zoé, with a ZE40 battery. This is an EV with a Power-Train (PWT) consisting of a 68kW wound-rotor synchronous Electric Machine (EM), with a single-gear transmission which connects it to the rear wheel. The vehicle is powered by a 41kWh lithium-ion 400V battery. An inverter ensures the electric coupling between the battery and the electric machine. Fig. 1 presents the EV configuration.
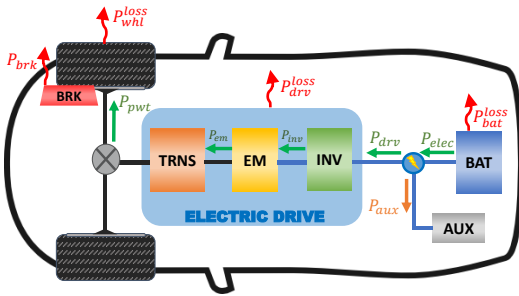

Fig. 1. EV Powertrain considered

Given that the goal of our study is to analyze energy losses due to the different transformations and also energy storage in the vehicle in the form of either kinetic or potential energy, the equations are arranged according to their role and / or their nature. To model EV energy consumption, we used the modeling framework presented in Guzzella et al. (2007), adapting it to data availability. The model parameters were given to us by Renault SAS.

2.1 Vehicle

For this model, we consider that positive-sign energy coming from the PWT and applied to the vehicle can be either stored in the vehicle mass in the form of kinetic and / or potential energy or "consumed" in order to propel the vehicle, by overcoming vehicle drag due to aerodynamic forces, rolling resistance, and other kinds of efforts (Guzzella et al. (2007)). In certain situations, the kinetic or potential energy already stored in the vehicle can be either extracted by the PWT and / or the brake system or used to propel the vehicle. We will denote P_{veh} the sum of the power coming from the PWT, P_{pwt}, either positive or negative, and the power used by the brakes, $P_{brk} \geq 0$, chosen as convention.

Given a vehicle speed, V_{veh}, the forces acting on the vehicle are an image of the energy exchange. Therefore, we have preferred to express the energy distribution as a force balance, as shown in (1). We can find the power associated to each force as $P_i = V_{veh} F_i$, for any force i present in (1).

$$F_{veh} = F_{pwt} - F_{brk} = F_{accl} + F_{slp} + F_{res}, \qquad (1)$$

where F_{accl} is the force necessary to accelerate the vehicle, F_{slp} the force caused by gravity on non-zero slopes and F_{res} is the total force; these forces are respectively associated with kinetic energy, potential energy and the energy needed for the vehicle to advance. They are calculated using equations (2,3,4).

$$F_{accl} = M_{veh}^{eq} \cdot \mathrm{d}V_{veh}/\mathrm{d}t = M_{veh}^{eq} \cdot a_{veh}, \qquad (2)$$

$$F_{slp} = M_{veh} \cdot g \cdot \sin\alpha, \qquad (3)$$

$$F_{res} = c_r \cdot M_{veh} \cdot \cos\alpha + \frac{1}{2} \cdot SCx \cdot \rho_{air} \cdot V_{veh}{}^2 + F_d, \quad (4)$$

where M_{veh} is the vehicle mass, g the acceleration due to gravity, α the road slope (in radians), c_r the rolling friction coefficient that depends on V_{veh}, SCx the product of the vehicle's cross-sectional area by the drag coefficient, ρ_{air} air density and F_d a disturbance force representing all non-considered phenomena. Finally, M_{veh}^{eq} is the equivalent mass of the vehicle, considering all rotational parts linked to the PWT.

2.2 Electric Drive

The Electric Drive (EDv) is the association of the inverter, the EM and the single-gear transmission (Fig. 1). Its function is to convert the electric energy coming from the battery into mechanical energy going to the wheels, and vice versa. For our study we modeled the EDv losses as a function of EM torque, T_{em} and rotational speed, ω_{em}. The relation between T_{em} and ω_{em} to F_{veh} and V_{veh}, is respectively given by $T_{em} = (R_{whl}/r_{trsm}) \cdot F_{veh}$ and $\omega_{em} = (r_{trsm}/R_{whl}) \cdot V_{veh}$; where R_{whl} is the wheel radius and r_{trsm} is the transmission ratio (including the differential gear).

In order to calculate the total power losses associated with EDv, P_{drv}^{loss}, we used a loss look-up table, which takes as input the EM torque and rotational speed, and the battery voltage (which is the EDv input), U_{bat}. Energy losses depend on U_{bat} as inverter efficiency may vary according to its input voltage. Considering the effect of U_{bat} allows us to take into account the effect on EDv efficiency of battery State of Charge (SoC) and of battery voltage drop or rise depending on power demand. Equation (5) is used to calculate EDv total input power, P_{drv}, and (6) presents P_{drv}^{loss} calculation.

$$P_{drv} = P_{pwt} + P_{drv}^{loss}, \qquad (5)$$

$$P_{drv}^{loss} = f(\omega_{em}, T_{em}, U_{bat}), \qquad (6)$$

EDv torque limitation depends on both ω_{em} and U_{bat}, and is given by $\check{T}_{em}(\omega_{em}, U_{bat}) \leq T_{drv}^{loss} \leq \hat{T}_{em}(\omega_{em}, U_{bat})$.

2.3 Battery

The EV battery is represented by using an internal resistance model as presented in Guzzella et al. (2007). It means that we will suppose that battery dynamics are negligible. As shown on Fig. 1, the battery provides power for both the electric drive and the electric auxiliaries, including the air-conditioning system. This power will be denoted $P_{elec} = P_{drv} + P_{aux}$, where P_{aux} corresponds to auxiliaries electric consumption. In this study it is assumed that $P_{aux} = 0$.

In charge as in discharge, part of the energy respectively entering or leaving the battery is lost due to chemical and electrical phenomena. We will denote the associated power as P_{bat}^{loss}. Then we can define effective battery power P_{bat} as

the variation in the amount of energy stored in the battery, and calculate it thanks to (7). P_{bat}^{loss} can be calculated by using (8), where i_{bat} is battery current and R_{bat} is battery resistance, which depends on battery State of Charge SoC, on battery temperature θ_{bat}, and on whether the battery is in charge or discharge mode. Battery voltage can be calculated as $U_{bat} = OCV - R_{bat} \cdot i_{bat}$, and battery current as shown in (9), where OCV is battery open circuit voltage, and depends on SoC and R_{bat}.

$$P_{bat} = P_{elec} + P_{bat}^{loss} = P_{drv} + P_{aux} + P_{bat}^{loss}, \quad (7)$$

$$P_{bat}^{loss} = R_{bat} \cdot i_{bat}{}^2, \quad (8)$$

$$i_{bat} = \left(OCV - \sqrt{OCV^2 - 4P_{elec} \cdot R_{bat}}\right) / (2R_{bat}). \quad (9)$$

Finally, the variation in battery SoC can be calculated as $\mathrm{d}SoC/\mathrm{d}t = -i_{bat}/Q_{bat}$, where Q_{bat} is battery charge capacity.

2.4 Global Power Balance

By using the equations presented in this section, we can express variation in the amount of energy in the battery in terms of the different physical phenomena present in the vehicle, (10). As we can see, in traction, battery power can become either kinetic energy variation (P_{accel}) or potential energy variation (P_{slp}); it is used in electric auxiliaries (P_{aux}); or it is dissipated as losses due to vehicle movement (P_{res}), EDv operation (P_{drv}^{loss}) or battery operation (P_{bat}^{loss}). The same principle holds also for vehicle deceleration, including the power dissipated in the brakes (P_{brk}).

$$P_{bat} = P_{accl} + P_{slp} + P_{res} + P_{drv}^{loss} + P_{bat}^{loss} + P_{aux} + P_{brk}, \quad (10)$$

3. EQUIVALENT COMPARISON SETTING FOR ECO-DRIVING MANEUVERS

3.1 General Principle

First, given the fact that there are many divergent definitions of E-D in the literature, we present the definition used for our study: **Eco-driving is adopting an adapted driving style in order to reduce the energy consumption of a vehicle**. This definition is an adaptation of the one proposed in Saerens (2012).

This definition is broad enough to encompass most of the publications on E-D, while remaining specific enough to exclude some practices that we consider as independent of E-D, even if they may be complementary, such as Eco-routing, or reducing heater or air-conditioning. In other words, E-D is limited here to driving style, even if other practices, such as choosing a path with a variable relief, may affect what one should do in order to Eco-drive.

Next, it is important to note that there are many ways in which a driver can modify his driving style in order to reduce his vehicle energy consumption. In this study we consider two: the first way is applying SDn, as for example by driving in the slow lane on highways; the second one is DAV. There are some other strategies with an energy reduction potential (e.g. driving behind a truck in order to reduce vehicle drag), but they are beyond the scope of our work. SDn and DAV have been reported in the literature as being applied in field studies with experienced EV drivers (Neumann et al. (2015); Rolim et al. (2012); Günther et al. (2017)).

Our hunch is that SDn and DAV are strategies that can be applied independently. This affirmation is supported by the fact that EV drivers tend to report them separately (e.g. Neumann et al. (2015); Günther et al. (2017)), and also by the observation that, in certain traffic conditions, a substantial and extended SDn would not be socially acceptable, whereas DAV, by its transient nature, would be better tolerated. We therefore considered independently the potential of these strategies on reducing EV energy consumption.

In the simulations presented below, the values of some external parameters associated either to EV state or to road, were fixed as follows: $SoC(t_0) = 70[\%]$, $\theta_{bat} = 30[^\circ C]$ and $\alpha = 0[\%]$; these are usual operating values. We will consider the case of urban driving as it is the most common EV case. The presented result were obtained by using MATLAB-Simulink® (MATLAB (2016)).

3.2 Slowing Down (SDn)

In order to evaluate the potential of SDn for reducing energy consumption, it is necessary to define a setting where different choices of cruise speed are energetically and functionally equivalent. When the vehicle cruises at different speeds, kinetic energy is not the same. This fact is not taken into account in the present section as, on the one hand, it is associated with transitory phases that can be neglected when it is possible to have long cruising phases (as in an open highway), and on the other, transient phases are associated with driver aggressiveness so they will be partially considered on next section.

From a functional point of view, it is also necessary to consider that the same distance will be traveled regardless of the chosen drive speed. Thus, we should consider a normalized energy consumption $E_{d_{ref}}^i$, necessary to cover a reference distance, d_{ref}, with a given cruise speed, V_{sdn}^i, as shown in (11); where P_{bat}^i is the instantaneous power the battery must apply (or receive) to maintain the chosen speed. Imposing an equivalent covered distance also allows us to have an equivalent potential energy variation in non-zero slope scenarios.

$$E_{d_{ref}}^i = \left(d_{ref} \cdot P_{bat}^i\right) / V_{sdn}^i. \quad (11)$$

In the case of urban driving, the main constraints on vehicle speed are due to traffic and infrastructure; it limits the speed reduction that a driver can apply in SDn. Thus, we will consider that the minimum acceptable speed corresponds to a 20% reduction w.r.t. a road limit speed of $50 km/h$ ($\approx 13.88 m/s$); we will also consider three intermediate speeds in order to assess the dependence of energy losses on the chosen cruising speed. The displayed energies are the result of integrating different terms in (10) over the maneuver duration.

Energy consumption $E_{d_{ref}}^i$ is shown on Fig. 2, for five different choices of cruising speed. Fig. 2 also shows $\Delta E_{d_{ref}}^i$, the energy economy with respect to the more energy-demanding maneuver (whose consumption is $\hat{E}_{d_{ref}} = \max E_{d_{ref}}^i$); it can be calculated for the i-th maneuver as $\Delta E_{d_{ref}}^i = \hat{E}_{d_{ref}} - E_{d_{ref}}^i$. The energy values on Fig. 2 were normalized so that $E_{d_{ref}}^i = 100\%$. The d_{ref} value is unimportant as the plotted results are normalized.
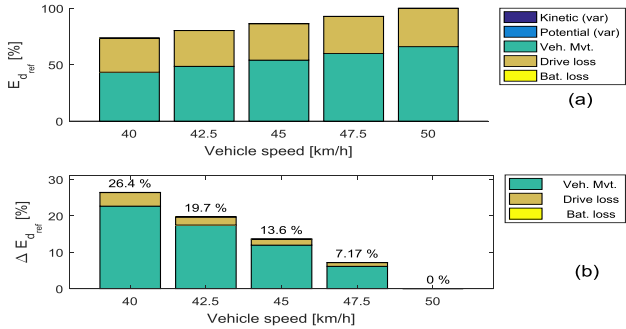
Fig. 2. Effect of SDn in energy consumption, on urban driving; (a) Absolute energy consumption [%], (b) Energy gain due to SDn [%]

Table 1. Energy gain distribution as a function of cruise speed, in urban driving

Source of losses	Vehicle speed [km/h]				
	40	42.5	45	47.5	50
Vehicle movement	85.7%	88.5%	87.7%	85.6%	-
EDv losses	14%	11.2%	12%	14.1%	-
Battery losses	0.254%	0.271%	0.285%	0.299%	-

Finally, it would be interesting to assess the contribution of each stage to the reduction in total losses, for each choice of cruise speed. For that, we have normalized energy economies for each cruise speed, so that the total energy economy associated to a given speed equals 100%. This is shown in Table. 1. This result confirms the natural intuition that most of the gains associated to SDn are due to a reduction in vehicle advance losses.

3.3 Driver Aggressiveness Variation (DAV)

Finding an energetically and functionally equivalent setting for evaluating the impact of DAV on energy consumption is not a trivial problem. For all maneuvers to be equivalent, there are two energetic constraints that must be respected, each associated with a functional constraint. First, we need to guarantee that the variation in the vehicle's kinetic energy is the same for the two maneuvers; it also means that the final speed will be the same for all maneuvers which corresponds to the fact that, SDn excluded, one tends to drive at the speed either imposed by traffic or legally authorized. Second, it is necessary to have the same variation in potential energy for each maneuver, which is associated (as a necessary condition) to the functional requirement of covering the same distance in each maneuver.

In order to meet these requirements we applied the approach used in Mruzek et al. (2017), formalizing it and applying it to acceleration and deceleration scenarios.

Acceleration Maneuvers   For acceleration maneuvers, we assume that the driver targets a final speed and, as soon as he reaches it, that he continues to advance at this speed (Saerens (2012), Mruzek et al. (2017)). This means that a fair way to compare two acceleration maneuvers would be to consider the consumption between the beginning of the maneuver and the moment when the distance covered by the fastest maneuver followed by a target-speed cruising phase equals the distance covered at the end of the slowest maneuver. For the sake of simplicity, in our study we will consider that the transitory phases take place at constant

acceleration. This is illustrated in Fig. 3, where the dashed line corresponds to the longest maneuver and the solid line to the i-th maneuver.
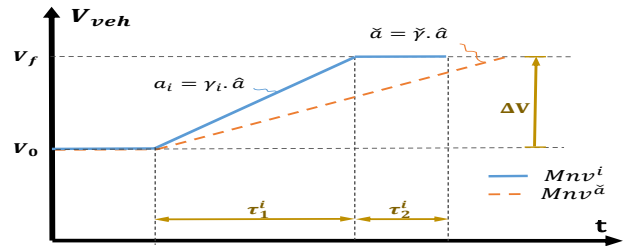

Fig. 3. Equivalent acceleration setting

Drivability constraints can be expressed in terms of the minimum acceleration that the driver would accept, $\check{a}$, and the acceleration that can be associated to a driver defined as "dynamical" (Javanmardi et al. (2017)), $\hat{a}$, respectively; these values were given to us for a certain number of driving situations by Renault SAS. In order to compare maneuvers in a systematic way, we will introduce the parameter $\gamma_i \in [\check{\gamma}, 1]$, which allows us to find the acceleration associated to the i-th maneuver, $a_i = \gamma_i \cdot \hat{a}$; γ_i serves as an indicator of driver aggressiveness in acceleration maneuvers. The longest maneuver is then associated to $\check{\gamma}$, with $\check{a} = \check{\gamma} \cdot \hat{a}$. By imposing $\check{\gamma} = \check{a}/\hat{a}$ we will guarantee that all maneuvers will respect the drivability constraints. Thus, the value of γ_i is an indicator of the maneuver aggressiveness during accelerations. We will respectively denote initial and final speed, V_0 and V_f, and the total variation in speed $\Delta V = V_f - V_0$. The duration of the acceleration and cruising-speed phases of the i-th maneuver are respectively τ_1^i and τ_2^i.

Once we have defined the maneuvers we want to compare, we have to find the cruising phase duration τ_2^i corresponding to the iso-distance constraint; this is done by applying (12). τ_1^i can be calculated as $\tau_1^i = \Delta V/(\gamma_i \cdot \hat{a})$.

$$\tau_2^i = \frac{\gamma_i - \check{\gamma}}{\gamma_i \cdot \check{\gamma}} \cdot \left(\frac{\Delta_V}{V_f \cdot \hat{a}} \right) \cdot \left(V_i + \frac{\Delta_V}{2} \right). \qquad (12)$$

We have considered $\gamma_i \in \{0.5, 0.625, 0.75, 0.875, 1\}$. The simulation results are presented on Fig. 4 and Table 2.
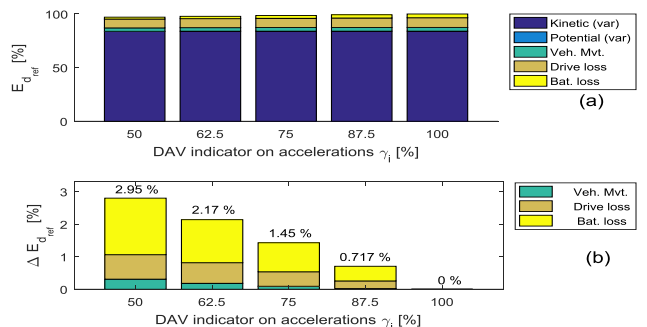

Fig. 4. Effect of DAV on energy consumption for acceleration maneuvers, in urban driving ($40 km/h \mapsto 50 km/h$); (a) Absolute energy consumption [%], (b) Energy gain due to DAV [%]

Deceleration Maneuvers   In the case of deceleration maneuvers, we will consider that an aggressive driver is one who does not anticipate deceleration phases. Therefore, we assume that he keeps a constant speed until the moment he decides to decelerate and that he then decelerates at a

Table 2. Energy gain distribution as a function
of DAV in accelerations, in urban driving

Source of losses	DAV indicator on acceleration γ_i [%]				
	50	62.5	75	87.5	100
Vehicle movement	11.1%	8.55%	6.43%	3.45%	-
EDv losses	26.9%	29.6%	31.2%	32.8%	-
Battery losses	62%	61.8%	62.4%	63.8%	-

constant rate. This is theoretically possible to achieve for a range of decelerations on vehicles that are equipped with an uncoupled brake pedal; however, the main goal of this analysis is to get a rough idea of how driver aggressiveness affects the energy consumption of the maneuver. It is important to point out that a driver's anticipation capacity on decelerations also depends on car-maker choice of pedal-off electric brake, so it would also give an idea of how this choice affects the minimum consumption potential of a given vehicle.

Fig. 5 presents the structure of a deceleration maneuver. As in the last section, drivability constraints are represented by a deceleration range, where $\hat{a} < 0$ is the maximum acceleration (minimum deceleration) and $\check{a} < \hat{a}$ is the minimum acceleration (maximum deceleration), . The parameter $\xi_i \in [\check{\xi}, 1]$ allows us to define the i-th maneuver deceleration, $a_i = \xi_i \cdot \check{a}$; ξ_i indicates driver aggressiveness during deceleration maneuvers, and is analogous to γ_j. By choosing $\check{\xi} = \hat{a}/\check{a}$, we guarantee the respect of drivability constraints. The longest maneuver is the one associated to $\check{\xi}$, with acceleration $\hat{a} = \check{\xi} \cdot \check{a}$. τ_0^i and τ_f^i are respectively the i-th maneuver cruise-speed phase and deceleration phase durations.
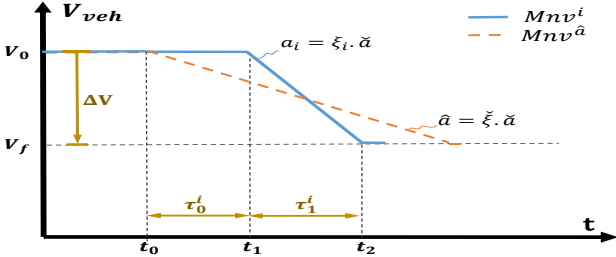

Fig. 5. Equivalent deceleration setting

The value of τ_0^i that respects the iso-distance constraint can be calculated by using (13). τ_1^i is given by $\tau_1^i = \Delta V/(\xi_i \cdot \check{a})$.

$$\tau_0^i = \frac{\xi_i - \check{\xi}}{\xi_i \cdot \check{\xi}} \cdot \left(\frac{\Delta_V}{V_0 \cdot \check{a}}\right) \cdot \left(V_i + \frac{\Delta_V}{2}\right). \qquad (13)$$

When decelerating, the amount of kinetic energy stored in the vehicle decreases, which means that $P_{accl} < 0$. Thus, this power could be used to charge the battery. A traditional bar-plot is not well-fitted to represent the energy balance of what has taken place during the maneuver. Therefore, we have chosen to use two superposed bar plots, where the widest one corresponds to kinetic energy (negative values), and the narrow bar plot corresponds to the other energy exchanges, and it starts at the end of the first bar plot. It is interesting to note that the difference between the two plots corresponds to the amount of vehicle kinetic energy that is transferred to the battery (as chemical energy) at the end of the maneuver.

It is also important to note that a normalized plot could be more difficult to define than for the previous cases,

given the fact that there are negative energy values. Thus, we have chosen to assign the value of 100% to $|P_{accl}|$, when $P_{accl} < 0$. In the general case of a nonzero slope, 100% corresponds to $|P_{accl} + P_{slp}|$, for $P_{accl} + P_{slp} < 0$, i.e., when the total energy stored in the vehicle mass at the end of the maneuver is less than at the begining. Thereby, the percent values presented on the (b) plots of Fig. 6, correspond to the percentage of $|E_{accl}|$ of the supplementary amount of energy of the i-th maneuver, w.r.t. the reference maneuver; $|E_{accl}|$ is the maximum amount of energy that, theoretically, could be sent from vehicle mass to battery during the maneuver.

For deceleration maneuvers, when driving in an urban setting, we will consider $\xi_i \in \{0.2, 0.4, 0.6, 0.8, 1\}$. The simulation results are presented on Fig. 6 and Table 3.
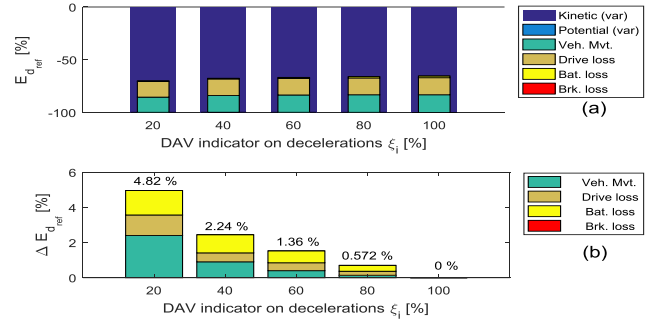

Fig. 6. Effect of DAV on energy consumption for deceleration maneuvers, in urban driving ($50km/h \mapsto 40km/h$); (a) Absolute energy consumption [%], (b) Energy gain due to DAV [%]

Table 3. Energy gain distribution as a function
of DAV in decelerations, in urban driving

Source of losses	DAV indicator on deceleration ξ_i [%]				
	20	40	60	80	100
Vehicle movement	48.4%	37%	26.2%	19.7%	-
EDv losses	23.5%	20.8%	29.4%	32.6%	-
Battery losses	28.1%	42.2%	44.4%	47.7%	-
Brake losses	0%	0%	0%	0%	-

3.4 Comparison of strategies

In the previous sections we analyzed the potential of different E-D strategies for reducing vehicle consumption, within a given driving scenario. However, it is also important to compare the different strategies in order to determine which are the most relevant in a given situation.

We present the consumption and gain associated to each strategy, for the different scenarios. In order to compare the different strategies fairly, we have normalized consumption to the same distance of 1km. Fig. 7 compares the potential of each strategy to reduce energy consumption; chart (a) presents the worst-case (dynamic driver) raw consumption associated to each urban driving scenario; chart (b) presents the energy economies associated to each E-D strategy, i.e. how much less energy is drawn from the battery (or how much more is stored there) by an Eco-driver compared to a dynamic one. As in the previous figures, all values have been normalized so that the maximum absolute value (on each graph) equals one.

As we can see on Fig. 7, the E-D strategy that has the greatest potential for urban driving scenarios is reducing aggressiveness in accelerations. This remarkable result is
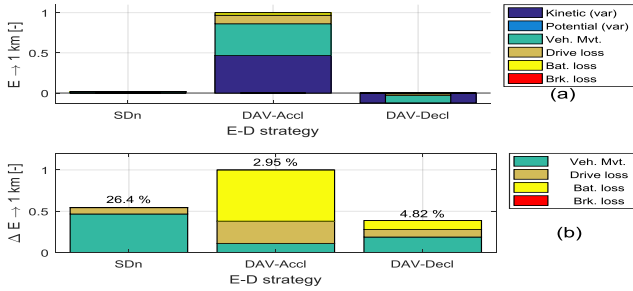
Fig. 7. Synthesis of E-D strategies potential, on urban driving ($40km/h - 50km/h$); consumption for 1 km; (a) Absolute energy consumption in the worst-case (dynamic driver), (b) Energy gain due to E-D (Eco-driver)

nevertheless coherent with some results reported in the literature (as in Mensing et al. (2014); Maamria et al. (2016)), where it is observed that the optimal strategy for urban settings consists in keeping a constant speed as much as possible. It is also coherent with the field study presented in Neumann et al. (2015), where it was found that DAV in accelerations and EV consumption are strongly partially correlated, whereas SDn and EV consumption are not significantly correlated.

It is also important to note that, quite surprisingly, most of the gains associated to DAV on accelerations are due to a reduction in battery and EDv losses. This can be explained by the fact that incrementing driver aggressiveness implies an increment in torque solicitation of the PWT. It implies both an increase in current, which reduces battery efficiency, and EDv operating at a less-efficient operating point.

4. CONCLUSIONS AND DISCUSSION

The comparison setting we have proposed has some advantages, e.g. the fact that all maneuvers are energetically equivalent, but there are also some issues associated to it as, for example, the fact that energy consumption depends on the choice of the longest maneuver for a given scenario. We think however that this disadvantage is largely compensated by the fact that it enables maneuvers to be compared fairly.

The results presented show that the best E-D technique in urban settings seems to be reducing driving aggressiveness in acceleration; however, the gains associated with SDn and DAV on decelerations are not negligible, so an Eco-driver should apply them all whenever the context allows him to do so. This information could even be applied on the design of real-time driving assistance functions.

For future studies, it could be useful to consider how variations in some parameters, such as road slope, battery temperature, and use of accessories (such as radio or air-conditioning systems), could affect what one should do in order to Eco-drive. It would also be useful to analyze E-D in highway settings, as it is probable that the E-D potential of different strategies may vary.

REFERENCES

Badin, F., Berr, F.L., Briki, H., Dabadie, J., Petit, M., Magand, S., and Condemine, E. (2013). Evaluation of evs energy consumption influencing factors, driving conditions, auxiliaries use, driver's aggressiveness. In *Electric Vehicle Symposium and Exhibition (EVS27), 2013 World*, 1–12. IEEE.

Dib, W., Chasse, A., Moulin, P., Sciarretta, A., and Corde, G. (2014). Optimal energy management for an electric vehicle in eco-driving applications. *Control Engineering Practice*, 29, 299–307.

Günther, M., Rauh, N., and Krems, J.F. (2017). Conducting a study to investigate eco-driving strategies with battery electric vehicles–a multiple method approach. *Transportation Research Procedia*, 25, 2242–2256.

Guzzella, L., Sciarretta, A., et al. (2007). *Vehicle propulsion systems*, volume 1. Springer.

Javanmardi, S., Bideaux, E., Trégouët, J.F., Trigui, R., Tattegrain, H., and Bourles, E.N. (2017). Driving style modelling for eco-driving applications. *IFAC-PapersOnLine*, 50(1), 13866–13871.

Maamria, D., Gillet, K., Colin, G., Chamaillard, Y., and Nouillant, C. (2017). Optimal eco-driving for conventional vehicles: Simulation and experiment. *IFAC-PapersOnLine*, 50(1), 12557–12562.

Maamria, D., Gillet, K., Colin, G., Chamaillard, Y., and Nouillant, C. (2016). On the use of dynamic programming in eco-driving cycle computation for electric vehicles. In *Control Applications (CCA), 2016 IEEE Conference on*, 1288–1293. IEEE.

MATLAB (2016). *version 9.1.0 (R2016b)*. The Math-Works Inc., Natick, Massachusetts.

Mensing, F. (2013). *Optimal energy utilization in conventional, electric and hybrid vehicles and its application to eco-driving*. Ph.D. thesis, INSA de Lyon.

Mensing, F., Bideaux, E., Trigui, R., Ribet, J., and Jeanneret, B. (2014). Eco-driving: An economic or ecologic driving style? *Transportation Research Part C: Emerging Technologies*, 38, 110–121.

Miyatake, M., Kuriyama, M., and Takeda, Y. (2011). Theoretical study on eco-driving technique for an electric vehicle considering traffic signals. In *Power Electronics and Drive Systems (PEDS), 2011 IEEE Ninth International Conference on*, 733–738. IEEE.

Mruzek, M., Gajdáč, I., Kučera, L., and Barta, D. (2016). Analysis of parameters influencing electric vehicle range. *Procedia Engineering*, 134, 165–174.

Mruzek, M., Gajdáč, I., Kučera, L., and Gajdošík, T. (2017). The possibilities of increasing the electric vehicle range. *Procedia engineering*, 192, 621–625.

Neumann, I., Franke, T., Cocron, P., Bühler, F., and Krems, J.F. (2015). Eco-driving strategies in battery electric vehicle use–how do drivers adapt over time? *IET Intelligent Transport Systems*, 9(7), 746–753.

Rolim, C.C., Gonçalves, G.N., Farias, T.L., and Rodrigues, Ó. (2012). Impacts of electric vehicle adoption on driver behavior and environmental performance. *Procedia-Social and Behavioral Sciences*, 54, 706–715.

Saerens, B. (2012). Optimal control based eco-driving. *Theoretical Approach and Practical Applications. Heverlee: Katholieke Universiteit Leuven*.

Sivak, M. and Schoettle, B. (2012). Eco-driving: Strategic, tactical, and operational decisions of the driver that influence vehicle fuel economy. *Transport Policy*, 22, 96–99.

Wahono, B., Santoso, W., Nur, A., et al. (2015). Analysis of range extender electric vehicle performance using vehicle simulator. *Energy Procedia*, 68, 409–418.